RSC Advances

ROYAL SOCIETY OF CHEMISTRY

www.rsc.org/advances

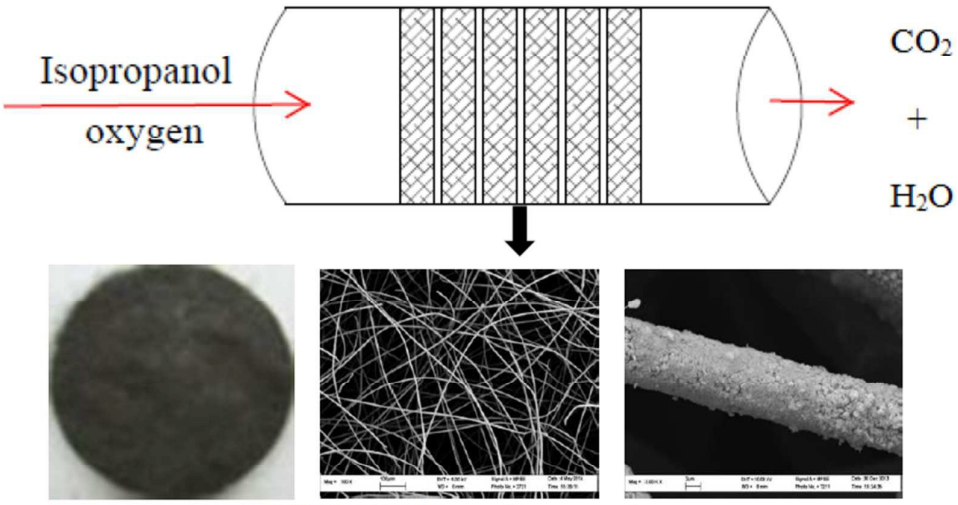

Mn/ZSM-5/PSSF membrane catalyst

Total oxidation of isopropanol over manganese oxides modified ZSM-5 zeolite membrane catalysts

Wang Ling, Zhang Huiping, Yan Ying, Zhang Xinya *

* *School of Chemistry and Chemical Engineering, South China University of Technology, Guangzhou 510640, PR China*

Abstract

Manganese oxides modified ZSM-5 membrane catalysts were prepared for the catalytic combustion of volatile organic compound (isopropanol) over a zeolite membrane reactor. Characterization of all samples was carried out by means of X-ray diffraction (XRD), scanning electron microscope (SEM), N_2 adsorption/desorption, X-ray photoelectron spectrum (XPS) and H_2-temperature programmed reduction (H_2-TPR). The performance of catalytic oxidation of single VOC (isopropanol) was investigated over the zeolite membrane reactor based on Mn/ZSM-5/PSSF catalysts, the experimental results showed that the 0.5 M Mn/ZSM-5/PSSF-350℃ catalyst exhibited the best catalytic activity for isopropanol oxidation with 90% conversion of isopropanol at 222℃with the feed concentration of 4.5 mg/L and GHSV of 7643 h^{-1}, which was much lower than that of granular Mn/ZSM-5 catalyst (297℃). The result of reaction stability test revealed that the Mn/ZSM-5/PSSF catalysts possess excellent reaction stability for isopropanol oxidation for 50 h, and the conversion of isopropanol remained above 97% at 280℃ with the feed concentration of 4.5 mg/L and GHSV of 7643 h^{-1}.

Key Words: Catalytic oxidation; Isopropanol; Stainless steel fibers; Manganese oxide; ZSM-5 zeolite membrane.

1. Introduction

Volatile organic compounds (VOCs) emitted mainly from industrial process and transportation activities can cause many health-related problems and environmental destructions[1,2,3]. Even in low concentration, VOCs may also pose severe threats to the human beings' health and the environment. The removal of VOCs is highly desirable. Catalytic oxidation method is recognized as a potent method of controlling emissions of VOCs owing to its low operating cost, low thermal emissions and high removal efficiency,[4,5]. At present, supported noble metals[6,7,8] and transition

* Corresponding author: Tel: +86 2087112047; fax: +86 2087112047.
E-mail address: cexyzh@scut.edu.cn (X.Y. Zhang).

metal oxides catalysts[9,10,11] are used for the reduction of VOCs emissions. Especially, transition metal oxides have shown an efficient catalytic performance in oxidation reactions, in addition, they offer lots of technical and commercial advantages that make them much better than noble metals[12,13].

Manganese oxides such as Mn_3O_4[14], Mn_2O_3[15] and MnO_2[16] are known for exhibiting high efficiency in the oxidation of VOCs and also considered as environmentally friendly materials[17]. The extensive catalytic application of these manganese oxides is due to their high efficiency in the reaction/oxidation cycles. Tseng and Chu[18] have reported that Mn/Fe_2O_3 was an excellent metal oxide catalyst in the catalytic oxidation of styrene. Sang et al.[19] found that the reactivity shows an order of $Mn_3O_4 > Mn_2O_3 > MnO_2$ in the oxidation of benzene and toluene, which was highly correlated with the oxygen mobility and the surface area of the catalysts, and the activity for VOCs combustion on manganese oxides is mainly determined by three factors: the surface area, the distribution of manganese states and active oxygen species (adsorbed oxygen, oxygen and lattice oxygen).

Support materials of the transition metal oxides are also considered as another important factor that determines the catalytic activity. Generally, zeolites[2,20,12], alumina[21,22], zirconia[23], titania[24] and silica[25] have been extensively applied as supports for preparation of VOCs oxidation catalysts. Zeolite supports have recently been paid much attention in the catalytic combustion of VOCs due to their large surface area, uniform and intricate channels, high adsorption capacity, high thermal and hydrothermal stabilities. However, the industrial application of these granular or powder catalysts have been limited because of the relatively high mass transfer resistance and bed pressure drop, as well as lower contacting efficiency exits in the traditional fixed bed reactor[26]. Recently, several structured supports such as aluminium foams[27], zeolite coated cordierite foams[26] and zeolite membrane-coated microreactor channels[28] which can well reduce these disadvantages have been widely applied in the preparation of catalysts that related to the combustion of VOCs. Zeolite membrane with obvious advantages of high specific surface area, uniform pore structure as well as good chemical stability has been well used for VOCs removal investigated in our group, which can well lessen the defects of traditional granular or powder catalysts[29].

The main projects of this research were to (1) prepare and characterize a well-designed novel porous catalyst containing manganese oxides supported on ZSM-5 membrane over paper-like

stainless steel fibers (PSSF); (2) investigate the catalytic activity of a series of Mn/ZSM-5/PSSF catalysts for isopropanol oxidation over a zeolite membrane reactor and (3) investigate the catalytic stability of the Mn/ZSM-5/PSSF catalysts for isopropanol oxidation over structured zeolite membrane reactor.

2. Experimental

2.1 Materials

Stainless steel fibers with an average diameter of 6.5 μm were purchased from Huitong Advanced materials Company (Hunan, China). Tetrapropylammonium hydroxide (TPAOH, 25% in water) was obtained from Sigma-Aldrich. Tetraethyl orthosilicate (TEOS, > 99%), isopropanol (> 99.5%) and the manganese nitrate ($Mn(NO_3)_2$, 50% in water) were purchased from Guangzhou Chemical Reagent Factory (Guangzhou, China). Ethanol (C_2H_5OH, > 99.8%) was purchased from Sinopharm Chemical reagent (Beijing, China).

2.2 Catalyst preparation

The novel porous ZSM-5/PSSF (paper-like stainless steel fibers) composites were synthesized by secondary growth process on the surface of PSSF (fabricated by wet lay-up papermaking and sintering process) according to the previous research in our group[29]. Then, manganese oxides modified ZSM-5/PSSF catalysts were prepared by wetness impregnation method, it involved the impregnation of 1.25g ZSM-5/PSSF composites with 30 mL aqueous solution containing knowing amounts of $Mn(NO_3)_2$ of 0.1, 0.25 and 0.5 M, the excess of water was removed in an oven at 100℃ until dryness, the as-synthesized samples were dried at 100℃ for 12 h and subsequently calcined in air for 4 h, the calcination temperature was adjusted at 350, 500 and 650℃.

2.3 Catalyst characterization

X-ray diffraction patterns (XRD) of samples were performed on a D8 Advance (Bruker Co.) diffractometer using Cu Kα radiation (40 kV, 40 mA). The diffractometer were recorded in the 2θ range of 5−80 ° with a 2θ step size of 1 ° and a step time of 10 s. The morphologies of the samples were observed by scanning electron microscopy (SEM, LEO-1530VP). Before analysis, all of the samples were coated with an ultrathin film of gold to make them conductive. The nitrogen adsorption and desorption isotherms were measured on a 3H-2000PS1 surface and pore size analyzer in static measurement mode at 77K. All samples were outgassed at 150℃ for 2 h before measurements. The specific surface area (S_{BET}) was determined by using the

Brunauer-Emmett-Teller (BET) method. The total pore volume was estimated by analyzing the N_2 adsorption-desorption isotherms, the mesoporous and microporous pore size distribution were obtained through BJH (Barrett-Joyner-Halenda)[30,31] and HK (Horvath-Kawazoe)[32] method, respectively. The X-ray photoelectron spectroscopy (XPS) measurements were obtained by using a Kratos Axis Ultra (DLD) spectrometer with an Al Kα (1486.6 eV) radiation source operated at 15 kV and 10 mA. The binding energy (BE) of the lattice O 1s peak at 529.9 eV was taken as a reference. H_2-Temperature programmed reduction (TPR) tests were conducted on Quantachrom Automated Chemisorption Analyzer by heating the catalyst in H_2 (10 vol%)/Ar flow (30 ml min^{-1}) at a heating rate of 10℃ min^{-1} from room temperature to 700℃. The hydrogen consumption was detected by thermo-conductivity detector (TCD). Before analysis, the samples were loaded into the reactor and purged with helium (30 ml min^{-1}) at 300℃ for 1 h to eliminate contaminants, and then cooled down to room temperature.

2.4 Catalytic test

Catalytic performance of Mn/ZSM-5/PSSF catalysts for isopropanol oxidation was evaluated in a continuous-flow fixed-bed reactor with a stainless steel tube (10 mm i.d., 450 mm length) under atmospheric pressure. The temperature of the catalyst bed and tubular electric furnace was monitored automatically by E-type thermocouples, respectively. In each test, the Mn/ZSM-5/PSSF catalyst were cut into circular disks (10 mm i.d) and placed coaxially in the reactor with a bed height of 1 cm. The continuous isopropanol gas was generated by bubbling air through the saturator, then further diluted with another air stream before reaching the reaction bed, the accurate flow rate of isopropanol gas was measured by mass flow controllers. An offline gas chromatograph (Agilent 7890A, Palo Alto, CA) equipped with a FID detector was used to analyze the VOC concentration in the feed and effluent streams. Before each test, the catalytic bed temperature was raised to 140℃ (no oxidation was detected) and stabilized for 30 min, then the catalyst bed was heated from 140℃ to 300℃ with a heating rate of 5℃/min, the reaction temperature was measured every 20℃ and each analysis was conducted after a stabilization time of 20 min at the desired temperature, analyses were made at least three times at each temperature and the results were finally averaged. The isopropanol conversion was calculated by the difference between inlet and outlet concentrations, the formula was described as follows

$$X_{VOC} = \frac{C_{VOC(in)} - C_{VOC(out)}}{C_{VOC(in)}} \times 100\% \quad (1)$$

Where $C_{VOC(in)}$ (mg/L) and $C_{VOC(out)}$ (mg/L) are the concentrations of VOC in the inlet and outlet, respectively.

3. Results and Discussion

3.1 X-ray diffraction

The XRD patterns of ZSM-5 zeolite membrane and different Mn/ZSM-5/PSSF catalysts with calcination temperature of 350, 500 and 650℃ are shown in Fig.1. All the XRD patterns in Fig.1 clearly present the diffraction peaks related to the PSSF (paper-like stainless steel fibers) materials at 2θ=43-55 °. Besides the diffraction peaks of PSSF, there are strong diffraction peaks which appear in the ranges of 2θ=7-9° and 2θ=23-25°, matching well with the standard patterns of ZSM-5 zeolite according to the literature[33]. For Mn/ZSM-5/PSSF catalysts, as revealed in Fig.1 (b-d), diffraction peaks that match with the diffraction patterns of manganese oxides are not significant in this paper. The relatively weak diffraction peaks at 2θ=32.9°and 65.8° in Fig.1 (d) may be ascribed to Mn_2O_3 (JCPDS:78-0390), these weak peaks corresponding to manganese oxides dispersed on surface of ZSM-5 membrane are possibly attributed to their well dispersion and small size, as was observed also in Zou's article[34].

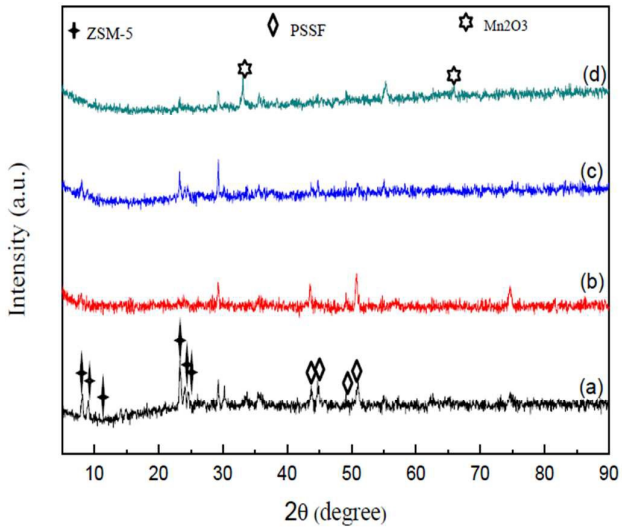

Fig.1. X-ray diffraction patterns of samples: (a) ZSM-5 zeolite membrane; (b) Mn/ZSM-5/PSSF-350℃; (c) Mn/ZSM-5/PSSF-500℃; (d) Mn/ZSM-5/PSSF-650℃.

3.2 SEM

Scanning Electron Microscopy (SEM) was used to analyze the microstructure and particle morphologies. Fig.2 shows the SEM micrographs of three-dimension network structure of stainless steel fibers support (a), the secondary growth of ZSM-5/PSSF (b), cross section of the ZSM-5 zeolite membrane (c) and the morphology of Mn/ZSM-5/PSSF catalysts (d-f). Fig.2 (a) clearly reveals that the junctures of stainless steel fibers are well sintered together to form a three-dimension network structure thus increasing the mechanical strength of the PSSF support. It can be seen in Fig.2 (b-c) that the ZSM-5 zeolite membrane grows well on the surface of the PSSF supports with a continuous dispersion and random orientation, the thickness of the ZSM-5 zeolite membrane is about 1.78 μm. In addition, the effect of calcination temperature on the morphology properties of the catalysts is represented in Fig.2 (d-f). As shown in the figure, the higher the calcination temperature, the more sintering and interaction of metal oxide species with ZSM-5/PSSF framework thus resulting in the decrease of active species on the catalyst surface. Moreover, with higher calcination temperature, the catalyst is crumbly and more cracks appear.

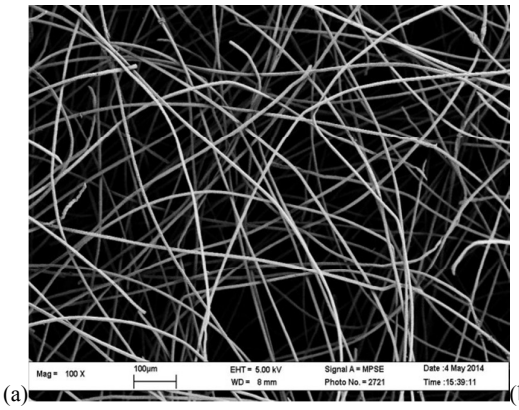

(a)

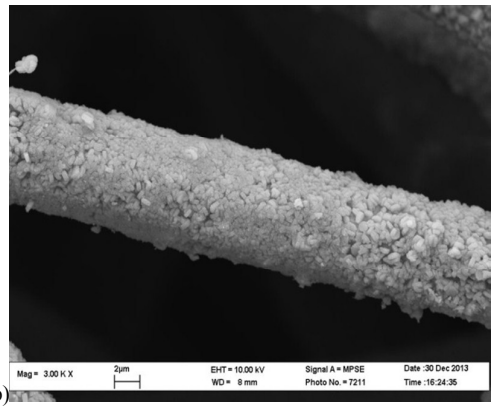

(b)

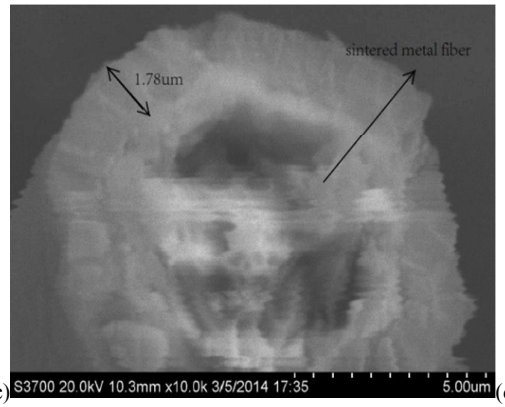

(c)

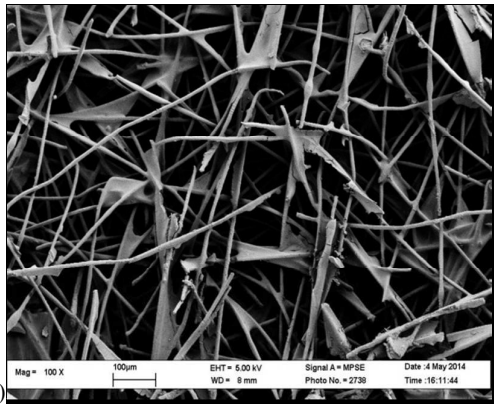

(d)

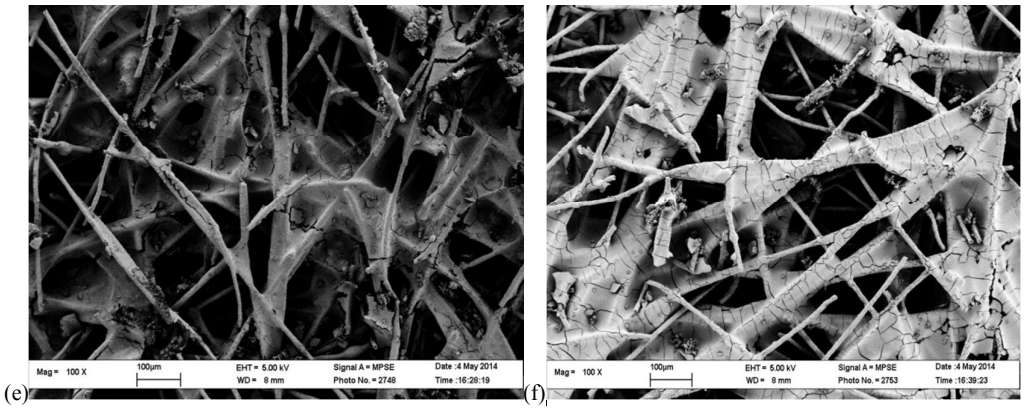

(e) (f)

Fig.2. SEM surface micrographs of samples: (a) three-dimension network structure of stainless steel fibers support; (b) ZSM-5/PSSF; (c) cross section of ZSM-5 membrane; (d) Mn/ZSM-5/PSSF-350℃, (e) Mn/ZSM-5/PSSF-500℃ and (f) Mn/ZSM-5/PSSF-650℃.

3.3 N_2 adsorption/desorption isotherms analysis

N_2 adsorption/desorption isotherms of ZSM-5/PSSF support and Mn/ZSM-5/PSSF catalysts were determined using 3H-2000PS1 instruments, as shown in Fig.3. The BET surface areas as well as the pore properties are summarized in Table 1. As can be seen in the Fig.3 (a-c), at the beginning, the volume adsorbed increased with the increase of relative pressure in the N_2 adsorption/desorption isotherms of ZSM-5/PSSF and Mn/ZSM-5/PSSF catalysts, which was due to the micropores of ZSM-5 zeolite membrane over the surface of PSSF. Fig.3 (b-d) clearly shows that the isotherms of Mn/ZSM-5/PSSF catalysts exhibit much larger hysteresis loops, which could be ascribed to the existence of mesopores between the particles of manganese oxides. As presented in Table 1, the BET surface area and total pore volume of PSSF are 11.98 m^2/g and 0.054 cm^3/g, respectively, the ZSM-5/PSSF support offers a relatively high BET surface area (105 m^2/g) and total pore volume (0.0621 cm^3/g). Besides, the calcination temperature had a significant effect on the BET surface area and total pore volume, the BET surface area and total volume both decreased with the increase of calcination temperature, the Mn/ZSM-5/PSSF-650℃ catalyst presents a much smaller BET surface area(13.24 m^2/g) and total pore volume (0.0186 cm^3/g) than the catalyst calcined at 350℃ with the BET surface area of 42.47 m^2/g and total pore volume of 0.0496 cm^3/g, respectively), which was ascribed to the sintering of the particles of the manganese oxides at relatively high calcination temperature[35], this result agrees well with the result of SEM.

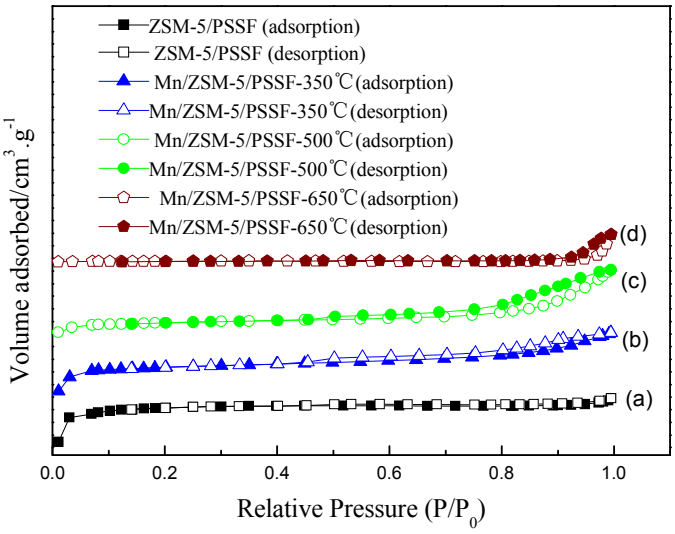

Fig.3. N_2 adsorption/desorption isotherms of samples: (a) ZSM-5/PSSF, (b) Mn/ZSM-5/PSSF-350℃, (c) Mn/ZSM-5/PSSF-500℃, (d) Mn/ZSM-5/PSSF-650℃.

Table 1 Pore structure characteristics of Paper-like Stainless Steel Fibers, ZSM-5 zeolite membrane and Mn/ZSM-5/PSSF catalysts.

sample	Micro-pore volume / $cm^3.g^{-1}$	Mesopore volume /$cm^3.g^{-1}$	Total volume /$cm^3.g^{-1}$	BET surface area S_{BET} /$cm^2.g^{-1}$
PSSF	--	--	0.0054	11.98
ZSM-5/PSSF	0.0397	0.0193	0.0621	105.00
Mn/ZSM-5(350℃)	0.0106	0.0305	0.0496	42.47
Mn/ZSM-5(500℃)	0.0096	0.0297	0.0439	33.77
Mn/ZSM-5(650℃)	0.0061	0.0192	0.0186	13.24

3.4 X-ray photoelectron spectroscopy (XPS)

The oxidation states of the constituent elements Mn and O ions in the synthesized catalysts were assessed by XPS measurements with an emphasis on the peaks associated with Mn 2p and Mn 3s, as shown in Fig.4. The surface element compositions of different catalysts are also summarized in Table 2. Fig.4 (A) presents the Mn 2p XPS spectra of Mn/ZSM-5/PSSF catalysts with different calcination temperatures, the Mn 2p spectra of all samples show two main asymmetric peaks at about 642.3 and 653.8 eV, which are corresponded to Mn $2p_{3/2}$ and Mn $2p_{1/2}$, respectively. An energy separation of 11.4-11.6 eV is observed between the Mn $2p_{3/2}$ and Mn $2p_{1/2}$ states. These results are in agreement with previous XPS spectra of Mn 2p reported by Todorova

et al[36]. The two peaks can be decomposed into two components at about BE=641.8 or 653.3 eV and 643.5 or 654.8 eV, the former is assignable to the Mn^{3+} species whereas the latter to Mn^{4+} species. The valence states of Mn could be illustrated by the splitting magnitude of Mn 3s XP spectra, which was shown in Fig.4 (B). As can be seen in the figure, the splitting energy of the 3s level on the Mn/ZSM-5/PSSF-350℃ catalyst is 4.9eV which is obviously lower than that on the Mn/ZSM-5/PSSF-650℃ catalyst (5.6eV). The higher splitting energy indicates that average oxidation state is lower, as was also observed in Tang's research[37].

In the case of photoemission from oxygen, the O 1s spectra shows two different surface oxygen species as displayed in Fig. 4 (C), where the asymmetric O 1s spectra is decomposed into two components for all the samples. The peak at lower binding energy of about 529.9 eV is characteristic of lattice oxygen ($O_{lattice}^-$) and the other peak at higher binding energy of about 531.9 eV is assigned to the surface adsorbed oxygen ($O_{adsorbed}$)[38,39]. According to the results of surface element composition in Table 2, the $O_{adsorbed}/O_{lattice}$ presents some difference between the Mn/ZSM-5/PSSF catalysts with various calcination temperatures, the decrease of $O_{adsorbed}/O_{lattice}$ probably could be ascribed to the sintering when increasing the calcination temperature. For the catalyst that calcined at 350℃, it presented the highest ratio of $O_{adsorbed}/O_{lattice,}$ which means that this kind of catalyst had the least amount of $O_{lattice}$, the oxygen vacancies would be relatively more, thus resulting in the intensive interaction between the absorbed molecules and electron on the surface of the support[40], and the Mn/ZSM-5/PSSF-350℃catalysts were supposed to have the best catalytic activity for isopropanol combustion.

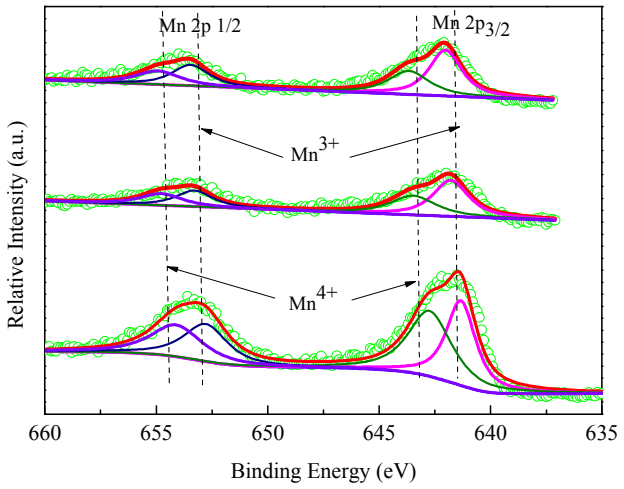

(A)

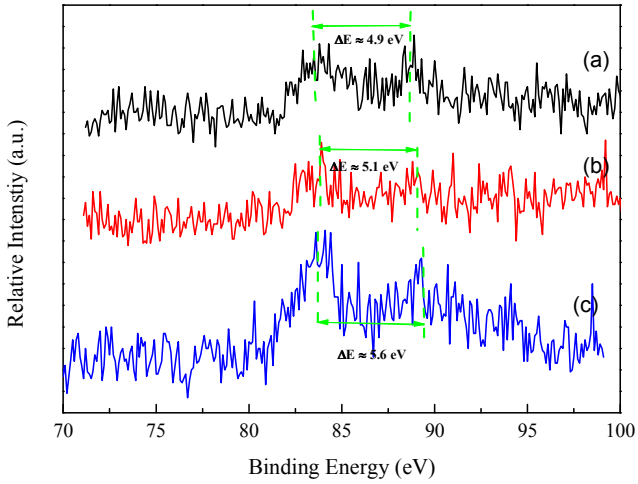

(B)

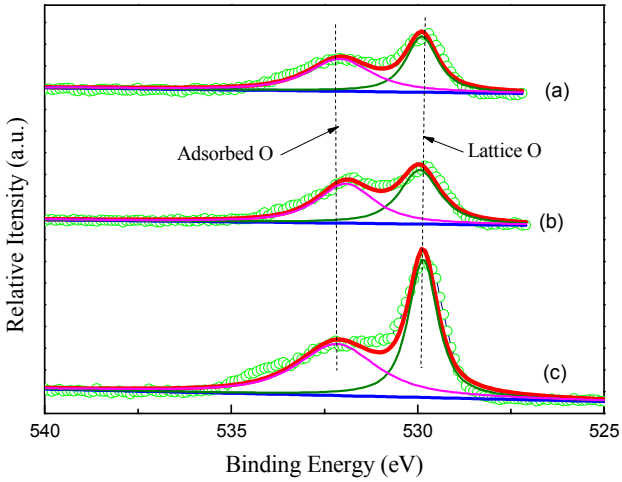

(C)

Fig.4 XPS analysis of (a) Mn/ZSM-5/PSSF-350℃, (b) Mn/ZSM-5/PSSF-500℃ and (c) Mn/ZSM-5/PSSF-650℃: (A) fitted Mn $2p_{1/2}$ and Mn $2p_{3/2}$ photoelectron peaks, (B) fitted Mn 3s photoelectron peaks and (C) fitted O 1s photoelectron peaks.

Table 2 Surface element composition of different catalysts

sample	Mn/ZSM-5/PSSF-350℃	Mn/ZSM-5/PSSF-500℃	Mn/ZSM-5/PSSF-650℃
$O_{adsorbed}/O_{lattice}$ [a]	1.16	1.04	1.01

[a] calculated from the XPS results

3.5 Temperature-Programmed reduction (TPR)

The reduction performances of Mn/ZSM-5/PSSF catalysts with different manganese loadings and calcination temperatures were investigated, the TPR profiles are shown in Fig.5 and Fig.6, respectively. As can be seen in the figures, all the catalysts presented two reduction peaks at the temperature range of 250-450℃, which corresponded to the reduction of MnO_2 to Mn_3O_4 and Mn_3O_4 to MnO[41,42], and the area ratio of former peak to the latter is about 2 in TPR profiles. After the experiments, the samples were green which matches well with the color of MnO. The reduction of MnO to Mn metal was not observed even up to a reduction temperature of 700℃ because of the large negative value of its reduction potential[43].

The reaction mechanisms are:

$$MnO_2 + \frac{2}{3}H_2 \rightarrow \frac{1}{3}Mn_3O_4 + \frac{2}{3}H_2O \quad (1)$$

$$\frac{1}{3}Mn_3O_4 + \frac{1}{3}H_2 \rightarrow MnO + \frac{1}{3}H_2O \quad (2)$$

However, the catalysts with different manganese loadings presented different TPR profiles with

different reduction temperatures, reduction rates and the shape of the peaks, as shown in Fig.5. As can be seen from the figure, the reduction peak temperature and H_2 consumption increased with the increasing of manganese loading. The higher reduction peak temperature was probably owing to the stronger interactions between manganese oxides and the support. According to the integral results of each curve, H_2 consumption increased from 8.39 to 37.47 with the increasing of manganese loading.

The calcination temperature also has a crucial effect on the reduction behavior of Mn/ZSM-5/PSSF catalysts, as revealed in Fig.6 (a-c). The onset of H_2 consumption started later as the calcination temperature increased. The two reduction peaks both shift to higher temperatures as the calcination temperature increased from 350 to 650℃, the reduction peaks are located at 297/384, 349/424 and 370/443℃, respectively, and the intensity of the peaks also weaken. For the catalyst calcined at 350℃, it presented a relatively sharp reduction peak at lowest temperature, the passible reason is that Mn exits in the form of MnO_2 which could be easily reduced. For the Mn/ZSM-5/PSSF-650℃ catalyst, the reduction peak at low temperature weakens greatly compared to the Mn/ZSM-5/PSSF-350℃ catalyst. At the calcination temperature of 650℃, Mn mainly exits in the form of MnO which is hard to be reduced, and the content of MnO_2 and Mn_3O_4 is relatively low. As for the catalysts calcined at 500℃, Mn exits in the form of MnO_2, Mn_3O_4 and MnO, so the reduction peak temperature lies in between the Mn/ZSM-5/PSSF-350℃ and Mn/ZSM-5/PSSF-650℃ catalysts. These results match well with the XPS result on manganese state distribution. On the other hand, the reduction peaks shifting to higher temperature is probably due to the lattice oxygen mobility on the catalyst, as was also observed in Sang's research[19]. The difference of hydrogen consumption within the catalysts that calcined at different temperatures could be explained by the reaction mechanism mentioned above, the H_2 consumption of MnO_2 is about twice as much as that of Mn_3O_4, so the hydrogen consumption of Mn/ZSM-5/PSSF-350℃ catalyst is the largest and the Mn/ZSM-5/PSSF-650℃catalyst had the lowest consumption level.

In addition, there is no obvious reduction peaks for the sample of ZSM-5/PSSF, as shown in Fig. 5(d) and Fig.6 (d), indicating that the ZSM-5/PSSF support is just considered as the perfect support and has no reduction properties.

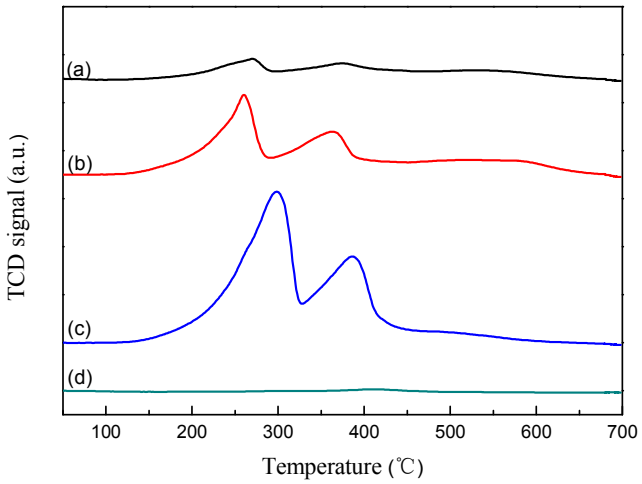

Fig.5. H_2-TPR profiles of Mn/ZSM-5/PSSF catalysts with different manganese loadings: (a) 0.1 M Mn/ZSM-5-350℃, (b)0.25 M Mn/ZSM-5-350℃, (c) 0.5 M Mn/ZSM-5-350℃ and (d) ZSM-5 zeolite membrane.

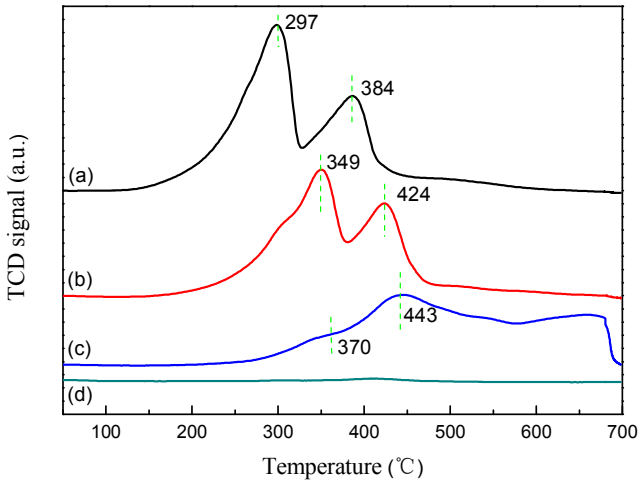

Fig.6. H_2-TPR profiles of Mn/ZSM-5/PSSF catalysts with different calcination temperatures: (a) Mn/ZSM-5-350℃, (b) Mn/ZSM-5-500℃, (c) Mn/ZSM-5-650℃ and (d) ZSM-5 zeolite membrane.

3.6 Catalytic performances

Catalytic performances tests for isopropanol oxidation over the catalysts with different metal loadings and calcination temperatures were carried out with a gas flow of 200 mL/min and inlet concentration of 4.5 mg/L over a structured zeolite membrane reactor, the conversion curves are shown in Fig.7. Fig.7(A) shows the effect of metal loading of Mn/ZSM-5/PSSF catalysts on the catalytic performances for isopropanol oxidation, as revealed in the figure, the synthesized catalyst with higher manganese loading (0.5 M Mn/ZSM-5/PSSF) presents better catalytic efficiency than

lower manganese loading catalysts (0.25 M Mn/ZSM-5/PSSF and 0.1 M Mn/ZSM-5/PSSF). The temperature of T_{50} and T_{90} are selected as parameters to demonstrate the catalytic activity toward isopropanol oxidation, as presented in Table 3, the values of T_{50} and T_{90} of isopropanol conversion decreased slightly with the increase of metal loading. According to T_{50}, the activity order of prepared catalysts is as follows: 0.1M Mn/ZSM-5/PSSF (230℃) < 0.25 M Mn/ZSM-5/PSSF (212℃) < 0.5 M Mn/ZSM-5/PSSF (207℃). Also, the activity order is the same at high isopropanol conversion (90%). The results indicate that the manganese loading of catalysts can influence the catalytic activity of isopropanol, the synthesized catalysts with high manganese loadings are more powerful for isopropanol combustion, the possible reasons are that ZSM-5/PSSF with high surface specific area and uniform microspores structure can adsorb more manganese ions under higher manganese concentration solution with the same impregnation time, and the catalyst with higher metal loading may offer much more active sites for isopropanol oxidation. Fig.7 (B) shows the effect of calcination temperature of Mn/ZSM-5/PSSF catalysts on the catalytic performances for isopropanol oxidation, as can be seen in the figure, the 0.5 M Mn/ZSM-5/PSSF catalyst calcined at 350℃presents a relatively high catalytic activity than the catalysts calcined at 500℃ and 650℃. These results match well with the results of XPS. For the catalyst calcined at 650℃, the catalytic activity is much lower and the catalyst possesses much higher T_{50} and T_{90}. For example, the catalyst calcined at 350℃ exhibits the lowest T_{50} (207℃) and T_{90} (233℃), which are much lower than the catalyst calcined at 500 ℃ (T_{50}=218℃, T_{90}=242℃) and 650℃ (T_{50}=240℃, T_{90}=275℃). The results indicate that the catalytic activity decreased with the increase of calcination temperature, these results matches well with the previous literature[44], as reported, the sintering of metal oxide species resulted in the decrease of active species on the catalyst surface when calcined the catalysts at much higher temperature.

Table 3 Temperature of 50% (T_{50}) and 90% (T_{90}) of isopropanol conversion over different catalysts with various operating conditions

catalysts	Manganese concentration (mol/L)	Calcination temperature (℃)	GHSV h^{-1}	Feed concentration (mg/L)	T_{50}(℃)	T_{90}(℃)
Mn/ZSM-5/PSSF	0.1	350	15286	4.5	230	257
Mn/ZSM-5/PSSF	0.25	350	15286	4.5	212	240

Mn/ZSM-5/PSSF	0.5	350	15286	4.5	207	233
Mn/ZSM-5/PSSF	0.5	500	15286	4.5	218	242
Mn/ZSM-5/PSSF	0.5	650	15286	4.5	240	275
Mn/ZSM-5/PSSF	0.5	350	7643	4.5	195	222
Mn/ZSM-5/PSSF	0.5	350	22929	4.5	210	237
Mn/ZSM-5/PSSF	0.5	350	15286	3.3	205	228
Mn/ZSM-5/PSSF	0.5	350	15286	10.4	208	240
GranularMn/ZSM-5	0.5	350	7643	4.5	248	297

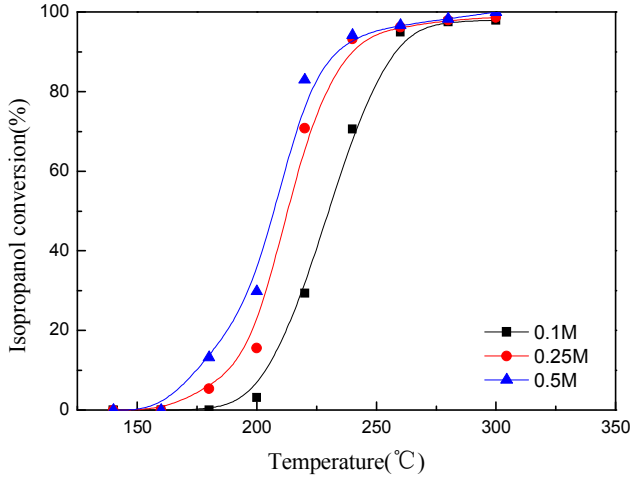

(A)

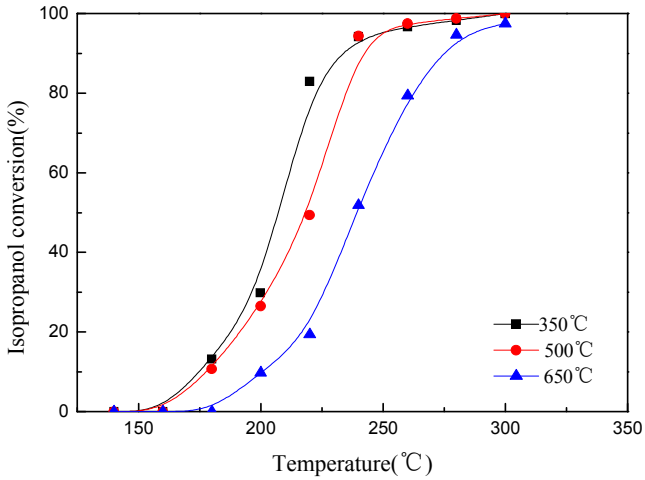

(B)

Fig.7. Catalytic performances for isopropanol oxidation over the Mn/ZSM-5/PSSF catalysts with different metal

loadings (A) (0.1, 0.2 and 0.5 M) and calcination temperatures (B) (350, 500 and 650℃). (4.5 mg/L of isopropanol in the feed gas and GHSV of 15286 h^{-1}).

The catalytic performances for isopropanol oxidation over the Mn/ZSM-5/PSSF catalyst (manganese loading of 0.5 M and calcination temperature of 350℃) were investigated using different inlet concentrations of isopropanol in the feed stream (3.3-10.4 mg/L) with a constant GHSV of 15286 h^{-1}. The conversion curves of the catalysts are given in Fig.8 (A) and Table 3. Table 3 shows that the T_{50} and T_{90} increase slightly as the inlet concentrations of isopropanol increase, the possible reasons are that more isopropanol molecules were adsorbed on the active sites in competition with oxygen at a high feed concentration, the surface oxygen was less and becomes the controlling factor, as a consequence, the conversion of isopropanol is lower, as was observed also in He's[4] and Ordonez's researches[45]. To investigate the effect of gas flow rate on the catalytic performance, experiments of isopropanol oxidation were conducted over the structured zeolite membrane reactor using different space velocity (7643~22929 h^{-1}) with a constant inlet concentration of isopropanol in the feed stream (4.5 mg/L). The catalytic performances for isopropanol oxidation are revealed in Fig.8 (B) and Table 3. Table 3 shows that the T_{50} and T_{90} increase slightly as the flow rates increase, the possible reasons are that the residence time of isopropanol molecules decreased in the zeolite membrane reactor at higher flow rates, which means the isopropanol molecules had little contact time with Mn/ZSM-5/PSSF catalysts when passing through the zeolite membrane reactor.

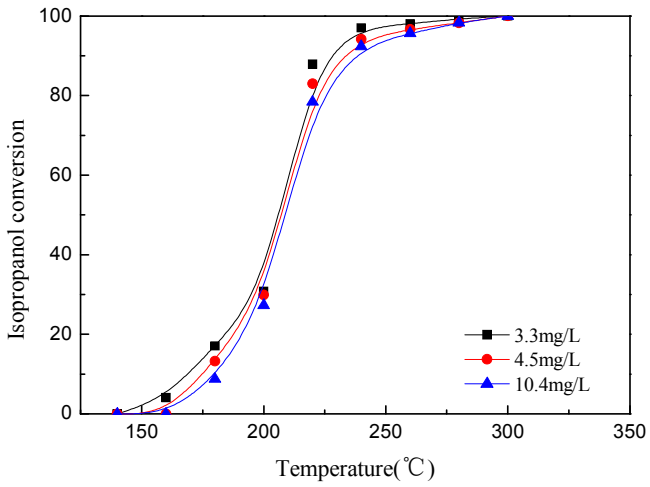

(A)

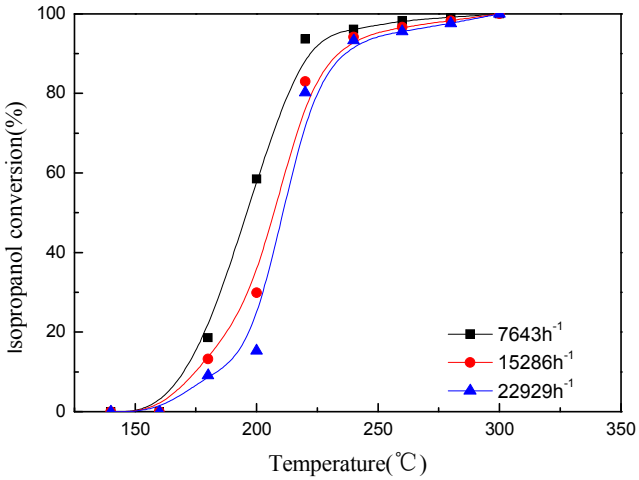

(B)

Fig.8. Catalytic performances for isopropanol oxidation over Mn/ZSM-5/PSSF catalysts (0.5 M of manganese concentration and 350 ℃ of calcination temperature) at different inlet concentrations (A) (3.3-10.4 mg/L) and different gas hourly space velocity (B) (7643-22929 h^{-1}).

The catalytic performances for isopropanol oxidation are also investigated based on granular Mn/ZSM-5 catalysts. Fig.9 shows the catalytic performance for isopropanol oxidation over the zeolite membrane reactor based on 0.5 M Mn/ZSM-5/PSSF catalysts and granular 0.5 M Mn/ZSM-5 catalysts (40-60 mesh) with a constant gas flow rate and feed concentration. As presented in the figure, the catalytic efficiency of Mn/ZSM-5/PSSF catalyst is superior to granular Mn/ZSM-5 catalyst, the Mn/ZSM-5/PSSF catalyst exhibit the T_{50} of 195℃ and T_{90} of 222℃, which are much lower than that of granular Mn/ZSM-5 catalyst (T_{50} =248℃ and T_{90} =297℃), as shown in Table 3. Also, 100% conversion of isopropanol could be achieved below 300 ℃ over Mn/ZSM-5/PSSF catalyst, while the isopropanol conversion is just near 92% over granular Mn/ZSM-5 catalyst at 300℃. The possible reasons are that ZSM-5 membrane on the PSSF supports can offer relatively lower mass transfer resistance than the granular ZSM-5, the internal diffusion resistance can be avoided in the Mn/ZSM-5/PSSF catalyst to a large extent, and the isopropanol molecules can pass through the catalysts bed more easily during the reaction, thus increasing the contacting efficiency between isopropanol molecules and catalysts.

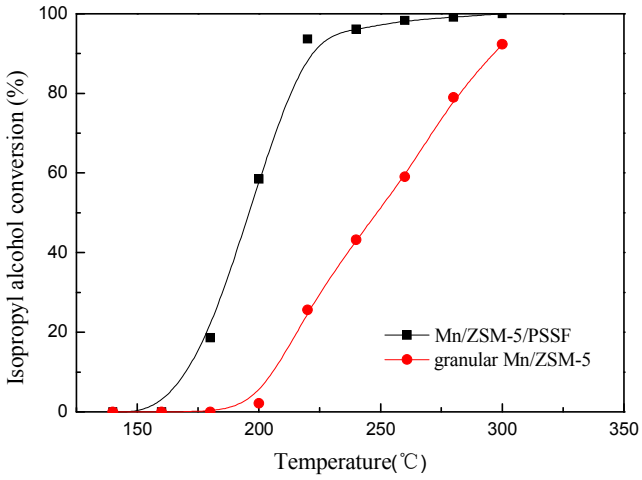

Fig.9. Catalytic performances for isopropanol oxidation over Mn/ZSM-5/PSSF catalyst and granular Mn/ZSM-5 catalysts. (0.5 M manganese concentration, 350℃ of calcination temperature, 4.5 mg/L of isopropanol in the feed gas and GHSV of 7643 h^{-1}).

In addition, the reaction stability test for isopropanol over Mn/ZSM-5/PSSF catalysts (manganese loading of 0.5 M, calcination temperature of 350℃) was carried out over the zeolite membrane reactor with a feed concentration of 4.5 mg/L , GHSV of 7643h^{-1} and reaction temperature of 280℃, the result is shown in Fig.10. The figure clearly indicates that the Mn/ZSM-5/PSSF catalysts possess excellent reaction stability for isopropanol oxidation, the conversion of isopropanol remains above 97% at 280℃ for 50 h. These results indicate that the Mn/ZSM-5/PSSF catalysts possess high catalytic activity and reaction stability for isopropanol oxidation.

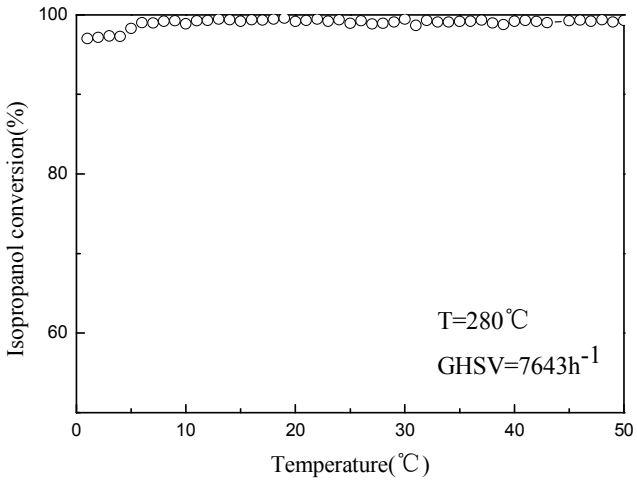

Fig.10. Reaction stability test for isopropanol oxidation over Mn/ZSM-5/PSSF catalysts (4.5 mg/L of isopropanol in the feed gas , GHSV of 7643 h^{-1} and reaction temperature of 280℃).

4 Conclusion

In summary, the manganese oxides modified ZSM-5 zeolite membrane catalysts Mn/ZSM-5/PSSF have shown excellent catalytic activity for isopropanol combustion, the conversion of isopropanol almost reached to 100% at 300℃. The characteristics of the catalyst were evaluated by XRD, SEM, N_2 adsorption/desorption, XPS as well as H_2-TPR method. The analysis results show that ZSM-5/PSSF appears as a promising catalyst support attributed to its high surface specific area and uniform microporous structure. The experimental results indicate that the 0.5 M Mn/ZSM-5/PSSF-350℃ catalyst exhibited the best catalytic activity for isopropanol oxidation at the feed concentration of 4.5 mg/L and GHSV of 7643 h^{-1}, demonstrated by a lowest T_{90} at 222℃, the catalytic activity is superior to granular Mn/ZSM-5 catalysts (T_{90} =297℃). In addition, the Mn/ZSM-5/PSSF zeolite membrane catalysts present excellent reaction stability for isopropanol oxidation in 50 h, isopropanol conversion remained above 97% at 280℃ with feed concentration of 4.5 mg/L and GHSV of 7643 h^{-1}.

Acknowledgements

Authors gratefully acknowledge the financial support from National Natural Science Foundation of China, Project Nos: 21176086 and 21376101.

References

1. N. Mukhopadhyay and E.C. Moretti, Centers for Waste Control Management, New York, 1993.
2. R. Beauchet, J. Mojoin, I. Batonneau-Gener and P. Magnoux, Applied Catalysis B: Environmental, 2010, 100, 91-96.
3. W.J. Ma, Q. Huang, Y. Xu, Y.W. Chen, S.M. Zhu and S.B. Shen, Ceramics International, 2013, 39, 277-281.
4. C. He, P. Li, J. Cheng, Z.P. Hao and Z.P. Xu, Water Air and Soil Pollution, 2010, 209, 365-376.
5. J.J. Li, J. Zheng, Z.P. Hao, X.Y. Xu and Y.H. Zhuang, Journal of Molecular Catalysis A: Chemical, 2005, 225, 173-179.
6. M.F. Luo, M. He, Y.L. Xie, P. Fang and L.Y. Jin, Applied Catalysis B: Environmental, 2007, 69, 213-218.
7. J. Maldonado-Hodar, Journal Hazardous Materials, 2011, 194, 216-222.
8. M. Ouamane and L.F. Liotta, Applied Catalysis B: Environmental, 2011, 101, 629-637.
9. J. Kugai, J.T. Miller, N. Guo and C.S. Song, Journal of Catalysis, 2010, 277, 46-53.
10. C. Gennequin, R. Cousin, J.F. Lamonier, S. Siffert and A. Aboukais, Catalysis Communications, 2008, 9, 1639-1643.
11. H.F. Li, G.Z. Lu, Q.G. Dai, Y.Q. Wang, Y. Guo and Y.L. Guo, Applied Catalysis B: Environmental, 2011, 102, 475-483.
12. T. Tsocheva, G. Issa, T. Blasco, M. Dimitrov, M. Popova, S. Hernandez, D. Kovacheva, G. Atanasova, J.M. Lopez-Nieto, Applied Catalysis A: General, 2013, 453, 1-12.
13. V.H. Vu, J. Belkouch, A. Ould-Dris and B. Taouk, Journal of Hazardous Materials, 2009, 169, 758-765.
14. M.V. Gallegos, L.R. Falco, M.A. Peluso, J.E. Sambeth and H.J. Thomas, Waste Management, 2013, 33, 1483-1490.
15. F.N. Aguero, A. Scian, B.P. Barbero and L.E. Cadus, Catalysis Letters, 2009, 128, 268-280.
16. S.M. Saqer, D.I. Kondarides and X.E. Verykios, Applied Catalysis B: Environmental, 2011, 103, 275-286.
17. A.H. Reidies, Ullmann's Encyclopedia of Industrial Chemistry, vol. A16. VCH, Weinheim, 1990, p. 123.
18. T.K. Tseng and H. Chu, Science of the Total Environment, 2001, 275, 83-93.
19. C.K. Sang and G.S. Wang, Applied Catalysis B: Environmental, 2010, 98, 180-185.
20. A.Z. Abdullah, M.Z. Abu Bakar and S. Bhatia, Industrial and Engineering Chemistry Research, 2003, 42, 5737-5744.
21. F.N. Aguero, B.P. Barbero, L. Gambaro and L.E. Cadus, Applied Catalysis B: Environmental, 2009, 91, 108-112.
22. R. Kikuchi, S. Maeda, K. Sasaki, S. Wennertrom and K. Eguchi, Applied Catalysis A: General, 2002, 232, 23-28.
23. Y.L. Gu, Y.X. Yang, Y.M. Qiu, K.P. Sun and X.L. Xu, Catalysis Communications, 2010, 12, 277-281.
24. V.H. Vu, J. Belkouch, A. Ould-Dris and B. Taouk, AIChE 2008, 54, 1585-1591.

25. H.Y. Pan, M.Y. Xu, Z. Li, S.S. Huang and C. He, Chemosphere, 2009, 76, 721-726.
26. F. Riberio, J.M. Silva, E. Silva, M.F. Vaz and F.A.C. Oliveira, Catalysis Today, 2011, 76, 93-96.
27. O. Sanz, F. Javier Echave, M. Sanchez, A. Monzon and M. Montes, Applied Catalysis A: General 2008, 340, 125-132.
28. N. Navascues, M. Escuin, Y. Rodas, S. Irusta, R. Mallada and J. Santamaria, Industrial and Engineering Chemistry Research, 2010, 49, 6941-6947.
29. H.H. Chen, H.P. Zhang and Y. Yan, Chemical Engineering Journal, 2012, 209, 372-378.
30. E.P. Barrett, L.G. Joyner and P.P. Halenda, Journal of American Chemistry Society, 1951, 73, 373-380.
31. L.G. Joyner, E.P. Barrett and R. Skold, Journal of American Chemistry Society, 1951, 73, 3155-3158.
32. G. Horvath and K. Kawazoe, Journal of Chemical Engineering of Japan, 1983, 16, 470-475.
33. M.M.J. Treacy and J.B. Higgins, Elsevier, 2001, 237.
34. Z.Q. Zou, M. Meng, L.H. Guo and Y.Q. Zha, Journal of Hazardous Materials, 2009, 163,835-842.
35. S.S. Jan, S. Nurgul, X.Q. Shi, H. Xia, Journal of Nanoscience and Nanotechnology, 2015, 15, 1-5.
36. S. Todorva, H. Kolev, J.P. Holgado, G. Kadinove, C. Bonev, R. Pereniguez and A. Caballero, Applied Catalysis B: Environmental, 2010, 94, 46-54.
37. W.X. Tang, X.F. Wu, G. Liu, S.D. Li, D.Y. Li, W.H. Li and Y.F. Chen, Journal of Rare Earths, 2015, 33, 62-69.
38. J.L.G. Fierro, Catalysis. Today, 1990, 8, 153-174.
39. L. Gonzalez Tejuca, A.T. Bell, J.L.G. Fierro and M.A. Pena, Applied Surface Science, 1988, 31, 301-316.
40. Z.Y. Tian, P.H.T. Ngamou, V. Vannier and K. Kohse-Hoinghaus, Applied Catalysis B: Environmental, 2012, 117-118, 125-134.
41. M. Ferrandon, J. Carno, S. Jaras and E. Bjornbom, Applied Catalysis A: General, 1999, 180, 141-151.
42. M. Wojciechowska, A. Malczewska, B. Czajka, M. Zielinski and J. Goslar, Applied Catalysis A: General, 2002, 237, 63-70.
43. R. Lin, W.P. Liu, Y.J. Zhong and M.F. Luo, Applied Catalysis A: General, 2001, 220, 165-171.
44. W.B. Li, W.B. Chu, M. Zhuang and J. Hua, Catalysis Today, 2004, 93-95, 205-209.
45. S. Ordonez, L. Bello, H. Sastre, R. Rosal and F.V. Diez, Applied Catalysis B: Environmental, 2002, 38, 139-149.